

FORMATION AND COLLAPSE OF QUIESCENT CLOUD CORES INDUCED BY DYNAMIC COMPRESSIONS

GILBERTO C. GÓMEZ,¹ ENRIQUE VÁZQUEZ-SEMADENI,¹ MOHSEN SHADMEHRI,^{2,3} AND JAVIER BALLESTEROS-PAREDES¹

Received 2007 May 2; accepted 2007 July 15

ABSTRACT

We present numerical hydrodynamic simulations of the formation, evolution, and gravitational collapse of isothermal molecular cloud cores in spherical geometry. A compressive wave is set up in a constant sub-Jeans density distribution of radius $r = 1$ pc. As the wave travels through the simulation grid, a shock-bounded spherical shell is formed. The inner shock of this shell reaches and bounces off the center, leaving behind a central core with an initially almost uniform density distribution, surrounded by an envelope consisting of the material in the shock-bounded shell, which at late times develops a logarithmic slope close to -2 , even in noncollapsing cases. The central core and the envelope are separated by a mild shock. The central core grows to sizes of ~ 0.1 pc and resembles a Bonnor-Ebert (BE) sphere, although it has significant dynamical differences: its self-gravity is initially negligible, and it is confined by the ram pressure of the infalling material, thus growing continuously in mass and size. With the appropriate parameters, the core mass eventually reaches an effective Jeans mass, at which time the core begins to collapse. Thus, the core evolves from a stable regime to an unstable one, implying the existence of a time delay between the appearance of the core and the onset of its collapse, but due to its growth in mass, rather than to the dissipation of its internal turbulence, as is often believed. These results suggest that prestellar cores may approximate BE structures, which are, however, of variable mass and may or may not experience gravitational collapse, in qualitative agreement with the large observed frequency of cores with BE-like profiles.

Subject headings: ISM: clouds — ISM: evolution — ISM: structure — stars: formation — turbulence

Online material: mpeg animations

1. INTRODUCTION

The process by which a gas parcel (“core”) within a molecular cloud (MC) initiates a collapse leading to the formation of a star or group of stars remains loosely understood, especially the details of its dynamical evolution. Observations indicate that “pre-stellar” molecular cloud cores (i.e., those that do not yet contain a protostellar object, but that appear to be on route to forming it) have a density structure that resembles Bonnor-Ebert (BE) profiles (Ebert 1955; Bonnor 1956), being nearly flat in their central regions, while approaching the singular isothermal sphere (SIS) profile $n(r) \propto r^{-2}$ at large radii. “Stellar” cores (those already containing a Class 0 or Class I protostellar object), on the other hand, appear to have density profiles closer to that of the SIS throughout their volume (e.g., Alves et al. 2001; Caselli et al. 2002; Kirk et al. 2005; Lee et al. 2007; see also the reviews by Lada et al. 2007; di Francesco et al. 2007; Ward-Thompson et al. 2007 and references therein).

The line profiles and spatial distribution of molecular line observations provide further clues to the dynamics. For example, on the basis of observations of CS(3–2), CS(2–1), DCO⁺(2–1), and N₂H⁺(1–0), Lee et al. (2004) found a moderate fraction of prestellar cores (18 out of 70 in their Table 2) showing clear evidence of subsonic inward radial motions, at velocities of $v \lesssim 0.07$ km s^{−1}. Moreover, studies of individual starless cores have suggested that the radial velocity does not increase appreciably toward the center (Tafalla et al. 1998; Williams et al. 1999; Tafalla et al. 2004; Lee et al. 2007; Schnee et al. 2007). Those inward motions frequently extend to long enough distances from the cores’ centers (a few tenths of a parsec) that they seem inconsistent with

the “inside-out” collapse model of Shu (1977), since a central protostar should have had time to form by the time the rarefaction wave reaches those distances (di Francesco et al. 2007 and references therein).

A large number of theoretical studies have investigated the collapse process starting from a variety of initial and boundary conditions, both analytically, through similarity solutions, and numerically (e.g., Larson 1969; Penston 1969a, 1969b; Shu 1977; Hunter 1977; Foster & Chevalier 1993; Hennebelle et al. 2003). All of these studies have considered the collapse of a *fixed* mass of gas, either through the usage of a hot, tenuous confining medium that pressure-confines the core while adding no weight to it, or through fixed boundaries. Moreover, most of these studies used static initial configurations, either with uniform density or with BE hydrostatic equilibrium profiles.

On the other hand, MCs are thought to be supersonically turbulent, since they exhibit supersonic line widths (Zuckerman & Palmer 1974), and MC cores, as well as their parent MCs themselves, have been suggested to be turbulent density fluctuations within their environments (Sasao 1973; Elmegreen 1993; Ballesteros-Paredes et al. 1999b), being produced by effectively supersonic compressions. Hunter & Fleck (1982) showed that the effective Jeans mass of a fluid parcel subject to an external compressive velocity field is significantly decreased with respect to its normal static value. Furthermore, Vázquez-Semadeni et al. (2005) have recently pointed out that if MCs are isothermal throughout,⁴ then the hot, tenuous medium necessary to confine and stabilize a hydrostatic equilibrium configuration is not available, and the equilibrium state is then expected to be unstable in general.

This leads naturally to the question of whether hydrostatic equilibrium configurations can be produced in such turbulent conditions,

¹ Centro de Radioastronomía y Astrofísica, Universidad Nacional Autónoma de México, Morelia, Michoacán 58089, Mexico; g.gomez@astrosmo.unam.mx, e.vazquez@astrosmo.unam.mx, j.ballesteros@astrosmo.unam.mx.

² Department of Physics, School of Science, Ferdowsi University, Mashhad, Iran.

³ School of Mathematical Sciences, Dublin City University, Glasnevin, Dublin 9, Ireland; mohsen.shadmehri@dcu.ie.

⁴ The possibility that MCs may contain warmer atomic gas interspersed with the colder molecular gas has been recently raised by Hennebelle & Inutsuka (2006). If this turns out to be the case, then the argument against the feasibility of stable hydrostatic BE-like MC cores weakens significantly.

and if so, how do they arrive at that state? Otherwise, if the entire process is dynamic, one can ask, what is the density and velocity structure of the cores at the time they engage into collapse, and, if it is different from the initial conditions normally assumed, what effects does that have on the evolution? Moreover, if the core is formed and induced to collapse by a compressive wave, then in general there is an *inflow* that builds up the core dynamically, and the mass that ends up collapsing is not previously determined by the initial conditions, but rather is determined “on the spot,” depending on the local instantaneous conditions. The studies of collapse mentioned above cannot answer these questions, since they already assume gravitationally unstable structures and initial hydrostatic equilibrium configurations, so that all of the mass is involved in the collapse.

A study that comes close to these goals is that by Hennebelle et al. (2003), who investigated the effect of an increase in the pressure external to an initially stable BE sphere, P_{ext} . They noted that the resulting configurations are a good match to the observations because the density profile is flat at the center and the prestellar phase is characterized by subsonic inward velocities at the outskirts and by nearly zero velocity at the inner parts. However, having a hot confining medium outside and an initial hydrostatic profile, this study still could not capture the core *formation* part of the evolution, and it predetermined the mass that collapses from the initial conditions. Also, it did not consider the possibility of a transient compression and thus of a failure to collapse.

A brief discussion of the dynamic scenario of core formation has been given by Whitworth et al. (2007) in the context of the formation of cores that give birth to brown dwarfs. These authors have suggested that the dynamic formation of cores should involve a mass growth period and the confinement of BE-like structures by ram pressure of external infalling material.

In view of the above, in this paper we then present numerical hydrodynamic simulations in spherical coordinates of transient compressions in homogeneous, initially gravitationally stable regions, with the purpose of investigating the formation of cores embedded in turbulent molecular clouds. In particular, we focus on the evolution of its density and velocity profiles, the time-scales required for a core to be assembled and then collapse or redisperse, and the mechanism by which a certain fraction of the mass is gravitationally “captured” to then proceed to collapse.

In particular, the timescale issue is highly relevant, because it is often thought that the prestellar lifetimes of the cores in the turbulent scenario of star formation are of the order of *one* core’s free-fall time, τ_{ff} . However, it has been shown by Vázquez-Semadeni et al. (2005) and Galván-Madrid et al. (2007) that even in highly dynamical, driven-turbulence simulations, the lifetimes are a few to several times τ_{ff} . It is important then to investigate the detailed evolution of cores formed by turbulent compressions, in order to understand the reason for those observed timescales.

The plan of the paper is as follows. In § 2 we first discuss the motivation and applicability of the spherical symmetry used in this paper, and then we describe the numerical setup of the problem. In § 3 we present the results of two fiducial cases of core evolution, one collapsing and one rebounding, and in § 4 we then discuss the implications of our results and compare with existing observational and theoretical work. Finally, in § 5 we present a summary and some concluding remarks.

2. THE MODEL

2.1. The Need for Focused Compressions

The formation and subsequent induction to gravitational collapse of clouds and clumps by compressive velocity fields (as opposed, in particular, to collisions of preexisting clouds) has

been studied intensively by numerous workers for more than three decades (e.g., Sasao 1973; Hunter & Fleck 1982; Tohline et al. 1987; McKee et al. 1993; Elmegreen 1993; Vázquez-Semadeni et al. 1996, 2003, 2005, 2007; Ballesteros-Paredes et al. 1999b; Ostriker et al. 1999, 2001; Klessen et al. 2000; Heitsch et al. 2001; Li et al. 2004; Tilley & Pudritz 2004, 2005). In such a scenario, the formation of cores and stars is in agreement with observational studies that suggest that star formation is a rapid and dynamic process (e.g., Lee & Myers 1999; Ballesteros-Paredes et al. 1999a; Elmegreen 2000; Pringle et al. 2001; Briceño et al. 2001; Hartmann et al. 2001; Ballesteros-Paredes & Hartmann 2007). The ability of a compression to induce collapse is directly related to the stability of self-gravitating equilibrium structures, which in turn depends critically on the geometry of the configurations and on the *effective polytropic exponent* (γ_{eff}) of the medium. This exponent describes the response to compressions of a medium subject to heating and cooling processes (Tohline et al. 1987; Elmegreen 1991; Vázquez-Semadeni et al. 1996), so that the flow exhibits an effective polytropic equation of state of the form $P \propto \rho^{\gamma_{\text{eff}}}$.

The stability of self-gravitating structures depends both on the geometry and on γ_{eff} because both of them influence the variation of the ratio $J^2 \equiv |E_g|/E_{\text{th}}$ in response to compressions, where $|E_g|$ is the absolute value of the gravitational energy and E_{th} is the (supporting) internal energy. For example, it is well known that the existence of stable *spherical* configurations without any external confining agent requires $\gamma_{\text{eff}} > 4/3$ (Chandrasekhar 1981, § 117). In this case, J^2 decreases on compression and increases on expansion, rendering the equilibrium stable. This behavior is reversed for $\gamma_{\text{eff}} < 4/3$, so equilibrium configurations are unstable in this case. We refer to the value of γ_{eff} at which the reversal occurs as the *critical value*, $\gamma_{\text{eff},c}$.

Now, if the compression occurs along ν directions, so that the density increases as L^ν , where L is the length scale along the direction(s) of compression, then the rate of variation of $|E_g|$ and of J^2 with the compression depends on ν and, as a consequence, the critical value of γ_{eff} also depends on ν . Specifically, one obtains (McKee et al. 1993; Vázquez-Semadeni et al. 1996)

$$\gamma_{\text{eff},c} = 2(1 - \nu^{-1}). \quad (1)$$

This recovers the value of $\gamma_{\text{eff},c} = 4/3$ for three-dimensional (e.g., spherically symmetric) compressions, as well as the well-known fact that planar compressions ($\nu = 1$) cannot induce collapse in isothermal flows ($\gamma_{\text{eff}} = 1$), since $\gamma_{\text{eff},c} = 0$ in this case. Equation (1) also shows that the induction of collapse in isothermal media requires compressions in more than two dimensions ($\nu > 2$).

These considerations show that useful insight can be gained from the analysis of spherically symmetric compressions, such as those assumed in this paper, since the compressions that induce the collapse of selected subregions of turbulent, isothermal molecular clouds need to be of dimensionality higher than 2. Such compressions are expected to be rare but still existent in general supersonic turbulent regimes, involving a certain degree of *focusing* (or *convergence*) of the flow. For example, Whitworth et al. (2007) appeal to the low but finite probability of such focused compressions to explain the scarcity of $\sim 0.01 M_\odot$ brown dwarfs.

Finally, note that these convergent flows are in principle different from a simple passing shock (which is essentially a planar compression), although the latter can also induce multidimensional compression when the shock has a finite transverse extent, producing a flattened structure that then can contract gravitationally in the transverse direction.

2.2. The Numerical Setup

In view of the above considerations, in this work we consider an idealized spherical cloud subject to an external compression wave. The simple spherical geometry allows us to focus on the basic phenomena related to the effects of the compression. Moreover, by considering a uniform density distribution and allowing the system to dynamically choose the amount of mass involved in the collapse, we avoid some of the restrictions that previous work has imposed on the evolution.

The hydrodynamic evolution of this setup was solved using ZEUS (Stone & Norman 1992), a finite-difference, time-explicit, operator-split hydrodynamic code. The calculations were performed on a one-dimensional spherical grid, with the domain spanning the range $0 \text{ pc} < r < 1 \text{ pc}$ with 1000 grid points spaced such that $\delta r_{i+1}/\delta r_i = 1.005$. This yields a spatial resolution of $\approx 3 \times 10^{-5} \text{ pc}$ at the inner boundary and $\approx 5 \times 10^{-3} \text{ pc}$ at the outer boundary. (Selected simulations were performed with a much higher resolution of 4000 grid points, and no significant differences were observed.) The boundary conditions are “reflecting” at $r = 0$ and “outflow” at $r = 1 \text{ pc}$. *No confining agents are used whatsoever* (neither closed boundary nor hot tenuous medium), implying that mass can freely leave the system, although it cannot enter. The absence of a confining agent attempts to emulate the situation of a density enhancement immersed in a much more extended medium at the same temperature.

All simulations started with a constant density distribution, an isothermal equation of state, and a temperature of $T = 11.4 \text{ K}$, which, with a mean particle mass of $\mu = 2.36 m_{\text{H}}$, yields an isothermal sound speed of $c_s = 0.2 \text{ km s}^{-1}$. This setup was perturbed by a compressive velocity pulse given by the relation

$$v(r) = \begin{cases} 0, & r < r_0 - dr_0, \\ -v_0 \sin\left(\frac{\pi}{2} \frac{r - r_0}{dr_0}\right), & r_0 - dr_0 < r < r_0 + dr_0, \\ -v_0 \sin\left(\frac{\pi}{2} \frac{r_1 - r}{dr_1}\right), & r_0 + dr_0 < r, \end{cases} \quad (2)$$

where v_0 and r_0 are parameters of the simulation, $dr_0 = 0.1 \text{ pc}$, $r_1 = [r_{\text{max}} + (r_0 + dr_0)]/2$, and $dr_1 = [r_{\text{max}} - (r_0 + dr_0)]/2$, with $r_{\text{max}} = 1 \text{ pc}$. A simple self-gravity module was also added to the code.

Our approach continues along the lines of simple, basic models that have explored the gravitational collapse of MC cores, from Larson (1969) and Penston (1969a, 1969b) to Hennebelle et al. (2003), which we have extended to include an initial velocity impulse, intended to mimic the random compressive motions expected in a turbulent medium. Nevertheless, the one-dimensional nature of the model, together with the adopted spherical geometry, makes this setup somewhat unphysical, as it restricts the nature of the compressible wave to spherical shells, and “turbulent” support in this model is present only as purely divergent motion, with no rotational component. A more realistic way of modeling the core formation process, albeit perhaps less amenable to detailed analysis, would be to perform full three-dimensional (3D) numerical simulations via random compressions of finite cross section generated by bulk motions of the gas, similarly to what has been done for the diffuse medium by Vázquez-Semadeni et al. (2007). We intend to pursue this in the near future, over the theoretical foundation laid out by the simple present study.

Another limitation introduced by the adopted geometry is the large mass of the collapsed core resulting from our simulations (cf. § 3.2). In a more realistic simulation, without the geometrical and symmetry restrictions, the collapsing system would probably

undergo fragmentation. Therefore, we see the collapsed objects generated in these simulations not as a single star, but as the precursors of small clusters.

3. THE SIMULATIONS

3.1. Spontaneous Collapse

In order to study the effect of velocity fields in inducing the collapse of molecular cloud cores, we first need to determine when they can collapse under the influence of their self-gravity alone. Because of the adopted spherical geometry (the usual Jeans analysis is applicable to sinusoidal perturbations in plane-parallel geometry), the critical density ρ_c and mass (which we refer to as the effective Jeans mass) at which the core collapses may differ slightly from the standard Jeans values, and so we determine them here numerically. We set $v_0 = 0$ and let the simulation run for 10 Myr with a series of different initial densities.

As the simulations are started, self-gravity causes the cloud to begin contracting, increasing its mean density (see Fig. 1). At some point, the pressure gradient in the inner parts stops this process, and the contraction is reversed (the cloud “bounces” momentarily). If the cloud’s mass is large enough, self-gravity takes over again, the expansion is also reversed, and the cloud collapses; otherwise, the expansion continues until the simulation ends. It is found that an initial density value of 160 cm^{-3} yields a collapsing core, while a 2% lower density does not; therefore, we take the critical density as $\rho_c = 160 \text{ cm}^{-3}$. At this density, the mass in our numerical box (of radius $R = 1 \text{ pc}$) is $M_{\text{box}}(\rho_c) = 39.1 M_{\odot}$. For comparison, the mean density for which the standard Jeans length equals the diameter of the numerical domain (2 pc) is $\bar{\rho} = \rho_J \equiv \pi c_s^2 / GL_J^2 = 125 \text{ cm}^{-3}$.

In light of this result, we define the *effective* Jeans mass as the spherical Jeans mass (i.e., a sphere with diameter equal to the Jeans length at mean density $\bar{\rho}$) times a fudge factor A so that the product equals the box’s mass at the empirical critical density:

$$\begin{aligned} M_{\text{J,eff}} &= A \frac{4\pi\rho_c}{3} \left(\frac{L_J}{2}\right)^3 \\ &= A \frac{\pi^{5/2}}{6} \left(\frac{c_s^2}{G}\right)^{3/2} \rho_c^{-1/2}, \end{aligned} \quad (3)$$

where G is the gravitational constant. By setting $M_{\text{J,eff}} = M_{\text{box}}$, we obtain $A = 1.45$. For comparison, the standard Jeans mass at ρ_c is $M_J = 27.0 M_{\odot}$, and the BE mass (Ebert 1955; Bonnor 1956) is $M_{\text{BE}} = 1.18 c_s^3 / (G^3 \rho_c)^{1/2} = 10.0 M_{\odot}$.

3.2. Cores Formed by Ram Pressure

Although a large number of simulations were performed, our discussion will focus on two of them that are, respectively, representative of noncollapsing and collapsing cases. We denote the simulation with the initial velocity impulse at $r_0 = 0.33 \text{ pc}$ as S1, while simulation S2 places the impulse at $r_0 = 0.67 \text{ pc}$. Both simulations have the same velocity amplitude ($v_0 = 0.4 \text{ km s}^{-1} = 2c_s$) and subcritical initial density ($112.7 \text{ cm}^{-3} \approx 0.7\rho_c$), meaning that in the absence of compressive motions, both simulations would simply expand away.

The evolution of simulation S1 is shown in Figure 2. This figure shows, respectively, as a function of radius, the density, the logarithmic slope of the density radial profile, the velocity, and the core’s mass (*solid line*) and Jeans mass (*dashed line*) inside the radius, in the four rows from top to bottom at selected times (*left to right columns*). Shortly after the starting time ($t \approx 0.28 \text{ Myr}$), a

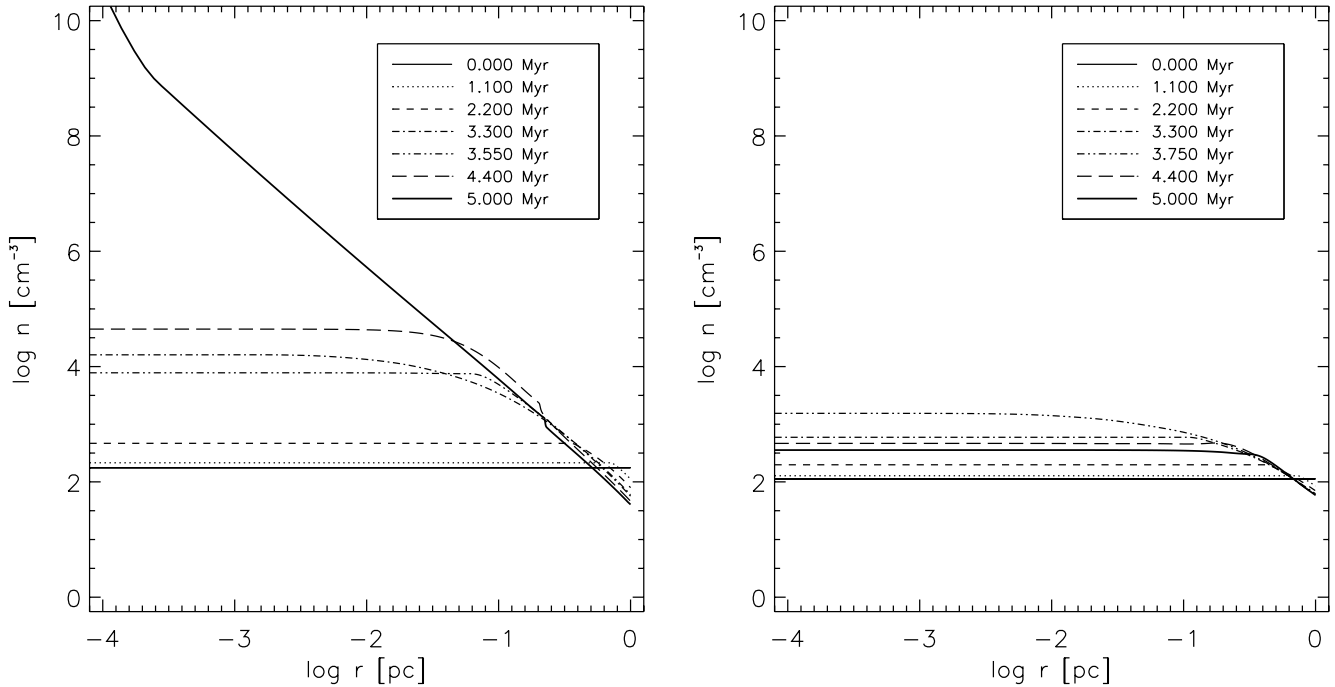


FIG. 1.— Spontaneous collapse of the cloud without any velocity impulse. *Left*: When started with a constant density of $n = 175.70 \text{ cm}^{-3}$, the central region of the cloud undergoes gravitational collapse after a small bounce off the center. *Right*: When started with a constant density of $n = 112.72 \text{ cm}^{-3}$, the cloud bounces off its center and expands until it disperses.

shell bounded by two shocks appears on the inner side of the initial velocity pulse, at $\log r \approx -0.7$ ($r \approx 0.2 \text{ pc}$). The formation of these two shocks and the shell between them is due to the middle parts of the compressive wave, which have the highest velocities, catching up with the frontal parts of the wave, causing the formation of a shock, which splits into two shocks receding from each other and leaving the shock-bounded layer in between.

The innermost one of these shocks propagates inward, leaving a large amount of inflowing mass behind it (Fig. 2b). As it travels toward the center of the cloud ($t \approx 0.77 \text{ Myr}$), geometrical focusing dramatically increases the internal density, lowering the effective Jeans mass of the inner parts of the cloud (Fig. 2c). As the shock bounces off the center and expands outward, the shocked gas behind it is left at uniform density and at essentially zero velocity; that is, a *quiescent core is formed*, with the shock-bounded shell doubling as the core's envelope (Fig. 2d). The gas from the shock-bounded shell continues to fall in, being incorporated into the quiescent core as it passes through the inner shock. Although the mass of the quiescent core increases, its density is somewhat lowered because of a mild expansion of the compressed region. As a result, the Jeans mass becomes larger in the innermost parts of the core and decreases close to the shock-bounded layer and within it (compare Figs. 2d and 2e). As the core acquires more mass, its density profile starts to deviate from being uniform and to approach that of a truncated BE sphere. However, in this simulation the mass of the inner core never becomes equal to $M_{J,\text{eff}}$ at any radius, and the uniform-density core begins to expand indefinitely, developing positive velocities at the outermost regions first (Fig. 2e).

In simulation S2, the early evolution is quite similar to that of S1. At $t \approx 1.5 \text{ Myr}$, the inner shock bounding the layer bounces off the center of the core (Fig. 3c) and begins traveling outward. But then, some 0.5 Myr later ($t \approx 2.0 \text{ Myr}$), the amount of mass in the core finally becomes equal to $M_{J,\text{eff}}$ (Fig. 3d) at $r \approx 0.07 \text{ pc}$, and from that moment on, collapse ensues, culminating with the formation of a singularity at $t \approx 2.6 \text{ Myr}$ (Fig. 3e). It is interesting

that at $t \approx 2.0 \text{ Myr}$, the mean density in the quiescent core is $n \approx 2.85 \times 10^4 \text{ cm}^{-3}$, implying a free-fall time of $\tau_{\text{ff}} \approx 0.2 \text{ Myr}$, less than half the time that the actual collapse takes. There are several reasons possibly responsible for the discrepancy with the observed collapse time of 0.6 Myr (from $t = 2 \text{ Myr}$ to $t = 2.6 \text{ Myr}$). For example, it was already noted by Larson (1969, Appendix C) that the actual collapse time lasts nearly 1.5 times the free-fall time, because the pressure gradient is never negligible. The remaining difference is probably due to the imprecisions introduced by considering the mean density rather than the detailed radial distribution and the fact that the core is increasing its mass, so that the instability sets in at an undetermined radius.

A very interesting feature of both simulations is the fact that the density structure of the core+envelope system resembles a BE sphere during the period over which the shock front is traveling outward (Figs. 2e and 3d), at which times the innermost parts of the core have a nearly constant density and the shock-bounded layer approaches an r^{-2} density profile. After the formation of the singularity at the center, the r^{-2} density profile extends throughout the core, similarly to an SIS profile (Fig. 3e).

It is worth remarking that, even though the idealized geometry and initial conditions adopted in this paper should not have a strong impact on the general qualitative behavior of these simulations, the sizes and timescales quoted above *are* expected to depend on these details. In fact, the outcome of the simulation (collapse or reexpansion) already depends sensitively on the parameters of our idealized simulations. For example, the only difference between simulations S1 and S2 is the initial position of the compressive pulse. Moreover, a simulation similar to S1 but started with $v_0 = 3c_s$ and a lower initial density (88.8 cm^{-3}) collapses 0.4 Myr after the initial shock bounces off the center. That is, a lower initial mean density can be counterbalanced by a larger compressive Mach number in the quest for inducing collapse. Nevertheless, this simulation still goes through the same qualitative evolution as simulation S2. For these reasons, the results presented in this section can be regarded as a qualitative

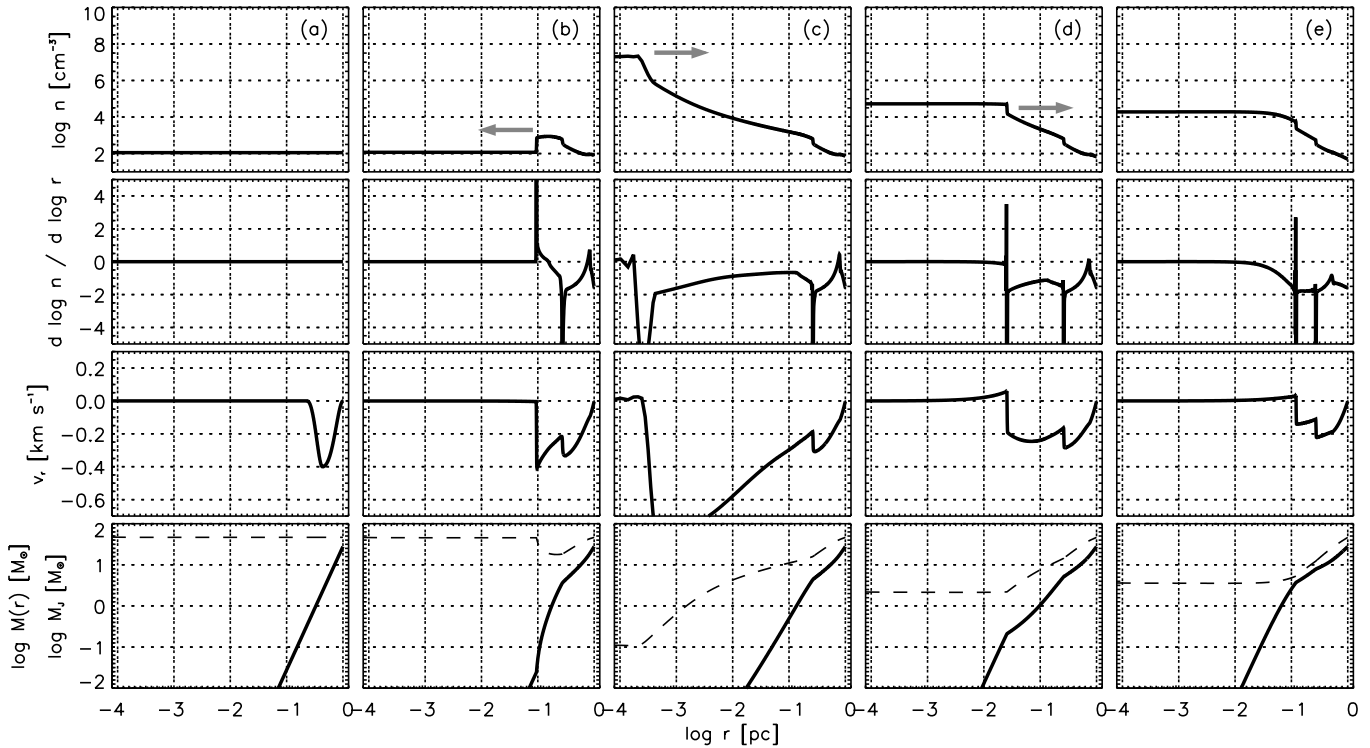


FIG. 2.—Evolution of simulation S1. Each row shows the evolution of (top to bottom) the density (n), the logarithmic density slope ($d \log n / d \log r$), the velocity (v_r), the mass internal to radius r [$M(r)$; bottom, solid line], and the effective Jeans mass ($M_{J,\text{eff}}$; bottom, dashed line) at (a) 0.000, (b) 0.625, (c) 0.775, (d) 0.925, and (e) 1.500 Myr. Arrows show the direction of motion of the shocks. [This figure is available as an *mpeg* animation in the electronic edition of the *Journal*.]

description of the formation and evolution of molecular cloud cores, while more quantitative analysis requires more realistic simulations involving multidimensional compressions, which we leave for future work.

4. DISCUSSION

4.1. Generality of Shock-bounded Self-gravitating Structures

The formation of *growing* shock-bounded structures is not exclusive to the spherical symmetry used in this paper. Planar compressions are generally known to produce shock-bounded layers in both isothermal and radiatively cooling flows. The one-dimensional plane-parallel problem is equivalent to that of a shock front hitting a wall and then reflecting off it, and thus by construction the gas between the wall and the shock is at rest, with the shock front receding from the wall at the postshock velocity of the flow. The shocked layer increases its mass as gas from the incoming flow is incorporated into it after crossing the bounding shock. The shock-bounded layer is thus the planar equivalent of our spherical shock-bounded quiescent core. The plane-parallel problem has been worked out analytically in one dimension and numerically in two or three dimensions by Folini & Walder (2006) for the isothermal case and by Hennebelle & Péroult (1999) and Vázquez-Semadeni et al. (2006) for the thermally bistable case. The main difference with the spherical case is that plane-parallel compressions in thermally bistable media (such as the warm H I gas) *can* induce gravitational collapse (Hunter et al. 1986; Vázquez-Semadeni et al. 2007), because in this case the flow behaves effectively as if it had a value of $\gamma_{\text{eff}} < 0$, while in an isothermal medium, focused (i.e., multidimensional) compressions are necessary, because in this case $\gamma_{\text{eff}} = 1$ (see § 2.1). However, the planar and the spherically symmetric cases are qualitatively similar in that both involve the for-

mation of a shock-bounded structure that grows in mass by accretion through the shock until it becomes gravitationally unstable and begins contracting. In the planar compression case, this process has been modeled numerically by various workers (e.g., Hunter et al. 1986; Vázquez-Semadeni et al. 2007).

4.2. Implications

The evolution of simulation S2 has a number of interesting important implications, which we now discuss.

First, a compressive wave (or a negative-divergence velocity field) does not directly induce the collapse of an initially sub-Jeans core. The collapse happens only if at some point in the evolution the mass becomes larger than the Jeans mass. In all the collapsing simulations we have performed here, this occurs only after the resulting shock front has rebounded off the center, traveled outward, and incorporated a large enough amount of mass into the central core that a “traditional” Jeans criterion for collapse [$M(r) > M_{J,\text{eff}}$] is satisfied there. Since the material behind the shock is left at zero velocity, *no turbulent support is ever at play there*. That is, the collapse does *not* occur because turbulence is dissipated in the core, as is often believed, but rather because the growing core eventually reaches the effective Jeans mass. Moreover, as the shock continues to move outward, the size of the region acquiring the effective Jeans mass increases, so the determination of the mass that is subsequently incorporated into the collapse happens “on the spot” in a highly fortuitous manner.

Second, a near- r^{-2} density profile is approached at late times in the infalling envelope around the central core, both in collapsing and noncollapsing cases. The central core, in turn, evolves from a near-flat density profile to that of a truncated BE sphere as its mass increases. The central core and the envelope are separated by the

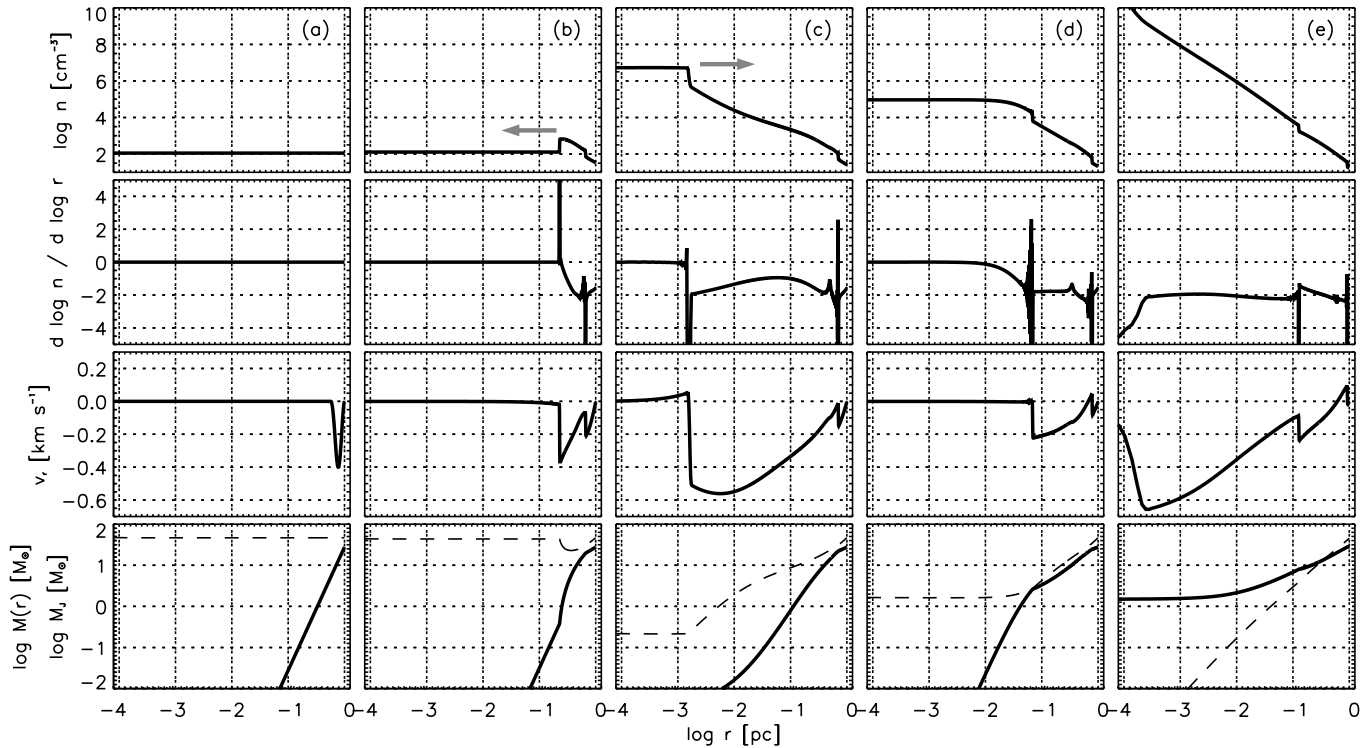


FIG. 3.—Same as Fig. 2, but for the evolution of simulation S2 at 0.000, 1.125, 1.525, 2.000, and 2.625 Myr. [This figure is available as an mpeg animation in the electronic edition of the Journal.]

outward-traveling shock, which is, however, very mild, with a Mach number very close to unity. Thus, the core+envelope system may easily be taken for a single structure with a density profile resembling that of a BE sphere.

Third, the central core, at all times after it has formed, has nearly zero velocity throughout. This provides a physical basis for the existence of quiescent (subsonic nonthermal velocity dispersion) and *coherent* (nonthermal velocity dispersion nearly constant through the core) cores, which in the turbulent model of core formation are the stagnation points of the turbulent flow in molecular clouds (Klessen et al. 2005).

Fourth, there is a time delay between the formation of the core and its gravitational collapse. The quiescent core grows from the center as the shock moves outward, incorporating mass into the central shocked region. This process cannot happen instantaneously, but rather requires a finite time until the core's mass equals the effective Jeans mass. In our simulations, the time from the moment of central core formation to the development of a singularity at the center spans roughly 1 Myr, with roughly half of it being spent without any tendency to collapse. This time delay naturally explains the high frequency of observed starless cores with BE-like profiles.

Fifth, it is important to remark that even though our quiescent cores are morphologically similar to BE spheres, they are dynamically very different: they are *not* confined by the thermal pressure of a hot, tenuous medium, but instead are confined by the ram pressure of the inflowing gas from the envelope and grow in size and mass accordingly until they become dominated by gravity, at which point they begin to collapse.

Sixth, and finally, it appears that the whole evolution is not very amenable to a similarity solution for the following reasons: (a) the initial velocity pulse is finite, so the external flow is not rescalable; (b) the inner shock bounding the shock-bounded shell

hits the center and bounces back toward the exterior, so the time of collision at the center breaks the self-similarity; and (c) the central core gradually increases its self-gravity and eventually may become gravitationally unstable, a process that continuously transforms the core's density profile from uniform to being BE-like, first stable and then unstable. Similarity solutions may be most applicable *after* the formation of the central singularity, as originally suggested by Shu (1977).

4.3. Comparison with Previous Work

It is interesting to put the results of our numerical simulations in context with those of previous studies. The main difference is that our simulations have investigated the *formation* of the cores, in addition to their subsequent collapse, in order to study whether BE-like structures can be spontaneously produced out of supersonic turbulent compressions in isothermal molecular clouds. Thus, in particular, our study sheds light on the realizability of the initial conditions used by previous works.

Our results suggest that in fully isothermal molecular clouds (i.e., without a warm, tenuous interclump medium that can stabilize a density enhancement), collapsing structures formed by random turbulent compressions in the medium morphologically resemble BE spheres through a large fraction of their evolution, because they consist of a central core and an infalling envelope, which, at late times after the formation of the central core, has a density profile with a slope close to -2 . This extends previous results stating that plane-of-the-sky angular averaging and line-of-sight averaging cause the *observed* density profiles to be smoother than the actual ones and thus easily confused with BE ones (Ballesteros-Paredes et al. 2003; Hartmann 2004). Also at late times, near the onset of gravitational collapse, the core also develops a density profile close to that of a BE sphere, which connects with that of the envelope. This means that, at the onset of

gravitational collapse, our simulations favor initial conditions for collapse such as those used by Foster & Chevalier (1993), albeit with the added ingredient of a continuous accretion at the bounding shock.

The establishment of a near- r^{-2} density profile in the envelope at late times is interesting in the context of the discussion by Shu (1977). He points out that the development of such a profile requires that the initial motions in the outer regions of collapsing cores be subsonic, so that all fluid parcels are in acoustic contact with each other and can therefore approach detailed mechanical balance. In our simulations, however, this need for an initially subsonic condition appears to be in contradiction with the supersonic nature of the initial pulse. However, the acoustic contact is restored in the envelope because it consists of shocked gas that has been thermalized and thus initially subsonic. The fact that a near- r^{-2} profile develops in the envelope even in the noncollapsing simulation can be understood because the compressive pulse effectively removes the support for the outer layers, analogously to the effect of an inside-out collapse.

Some authors have already studied spherically symmetric flows with shocks in the context of protostar formation using similarity methods (e.g., Shen & Lou 2004; Lou & Gao 2006; Lou & Wang 2006). Similarity studies are extremely useful in extracting the underlying asymptotic behavior of real flows. Therefore, it is important to compare our numerical solutions with existing similarity solutions of self-gravitating clouds in the presence of shocks, in particular those of Shen & Lou (2004, hereafter SL04), whose study most resembles our numerical setup. These authors presented two possible classes of self-similar shocked flow in the context of the dynamical evolution of protostars, depending on the asymptotic behavior of the solutions near the center of the cloud. Their Class I solutions had negative (inflow) velocities ($\propto -r^{1/2}$), a density profile of $\rho \propto r^{-3/2}$, and finite mass as asymptotic limits at $r \rightarrow 0$, while their Class II solutions had positive (expansion) velocities ($\propto r$), constant finite density, and vanishing mass ($\propto r^3$) as the asymptotic behavior in the same limit. In both classes, an outward-moving shock separates a collapsing (or expanding) inner part and an accreting outer part. None of these behaviors are seen in our simulations at any time. Their Class II solutions are similar to our solutions during the core-growth stage, in that they have a uniform central density and an accreting outer part, which has a counterpart in the infalling shock-bounded layer in our models. However, in our system the central core is neither expanding nor contracting, but rather it is at rest. This difference is most likely a consequence of self-gravity being negligible in our cores during the early stages of their evolution. That is, unlike the SL04 solution, where self-gravity is important at all radii and at all times, in our simulations the relative importance of self-gravity increases secularly with time, going from being zero at the time of core formation to being dominant at the time when gravitational instability sets in.

Another recent study that is closely related to ours is that by Hennebelle et al. (2003), who numerically investigated the effect of increasing the pressure external to an initially stable BE sphere, P_{ext} . These authors found that slow rates of increase of P_{ext} cause the sphere to approach instability quasi-statically, but higher rates of increase produced a compressive wave that triggers an outside-in collapse. It is noteworthy, however, that they do not report the bounce of the compressive wave from the center that we find. This is most probably because, in their case, the wave compresses a previously existing core that is in a (fragile) stable hydrostatic equilibrium state, and so the role of the wave is to directly trigger the collapse. Instead, in our case, the compressive wave *forms* the core and adds mass to it until it becomes gravitationally unstable and proceeds to collapse. Moreover, in the case of Hennebelle et al.

(2003), the mass of the core was fixed, being bounded by a hot, tenuous medium, while in our case, the fraction of the mass that is driven to collapse is determined “in real time” by the interplay between the accreting gas and the outgoing shock wave, and moreover, the mass that becomes gravitationally unstable increases with time, so the collapse proceeds “inside-out,” but over an intermediate range of radii. Thus, we see that the choice of equilibrium or out-of-equilibrium initial conditions and continuous or discontinuous boundary conditions leads to very different patterns of evolution. Which model applies best to actual turbulent molecular clouds probably depends on whether they consist of a single, nearly isothermal molecular phase (our model) or of a mixture of colder, denser molecular cloudlets immersed in a more tenuous and warmer atomic medium (Hennebelle & Inutsuka 2006). Extensive theoretical and observational work, focusing especially on the velocity structure of the cores, is needed to decide this issue. The recent results of Lee et al. (2007), indicating the presence of a sharp infall velocity increase at ~ 0.03 pc from the centers of the starless cores L694-2 and L1197, would seem to favor our dynamical scenario for the formation of the cores.

Finally, our results are fully consistent with the scenario outlined by Whitworth et al. (2007). These authors have foreseen the formation of evolving BE spheres bounded and fed by the accretion of external infalling material, which can collapse if the core eventually reaches the BE mass. Although they restricted their discussion to the formation of brown dwarf-producing cores, the simulations described here are seen to be applicable to the formation of cores of arbitrary mass. It is indeed likely that, as the core to be formed is of smaller mass, the required compression and focusing need to be stronger, as the initial conditions will have sizes much smaller than the local Jeans length (cf. § 3.2).

5. SUMMARY AND CONCLUSIONS

In this paper we have performed a numerical study of the formation of dense cores by dynamical compressions in isothermal, nonmagnetized media, using simple one-dimensional calculations in spherical geometry. Our results show that cores assembled by this process consist of a central, quiescent core with a density of 10^5 cm^{-3} that grows in mass and size as it accretes mass from a surrounding envelope. The quiescent core and the envelope are separated by a mild shock with a Mach number of just above unity, and the accretion from the envelope provides ram pressure that confines the central quiescent, growing core. As the central core increases its mass, it passes first through a negligible-gravity, uniform-density stage, and later, as self-gravity becomes important, it evolves into a “pseudo-BE sphere” stage. If at some point in the evolution the mass of the core + envelope system becomes larger than the Jeans mass, the core proceeds to collapse. Otherwise, it begins to reexpand. Even in collapsing cases, this process requires a relatively long time to complete, taking ~ 0.5 Myr from the first appearance of the central core to the time at which it becomes gravitationally unstable, and another ~ 0.5 Myr for the collapse to produce a singularity at the center.

At all times after the formation of the central core, the combined density structure of the core+envelope system resembles that of a BE sphere, since it is flattened at the center and has an outer density profile that approaches r^{-2} at late times. Moreover, the central core is quiescent at all times, except for during the very late stages of the noncollapsing case, in which the core begins to expand. Thus, the high observed frequency of BE-like profiles (e.g., di Francesco et al. 2007; Lada et al. 2007) and the quiescent/coherent velocity dispersion structure (Myers 1983; Goodman et al. 1998; Caselli et al. 2002; Tafalla et al. 2002, 2004; Schnee et al. 2007) is naturally accommodated in this

scenario of dynamic assembly of MC cores, as suggested also by studies of dense cores in turbulent simulations of 3D, isothermal molecular clouds (Klessen et al. 2005). However, the structures are not classical BE spheres, because they are confined by ram pressure, rather than by thermal pressure, and are consequently accreting mass and growing in mass, size, and self-gravitating energy in a process qualitatively similar to that described for the formation of giant MCs by Vázquez-Semadeni et al. (2007). In both cases, there is a secular evolution characterized by the mass increase of the cloud or core.

The velocity structure of the cores formed in our simulations appears to be consistent with the recent radiative transfer models for the structure of cores L694-2 and L1197 presented by Lee et al. (2007), which exhibit a nearly zero central velocity and a sharp rise at radii of ~ 0.03 pc. We plan to carry out a radiative transfer study of the density and velocity structures produced by our models in the

near future, in order to perform detailed comparisons with observational studies based on multitracer studies (e.g., Lee et al. 2004), as well as on line-profile mapping of prestellar cores (e.g., Tafalla et al. 1998, 2004; Lee et al. 1999, 2007; Schnee et al. 2007).

We wish to thank S. Lizano and an anonymous referee for useful comments. This work has received financial support from CRYA-UNAM to G. C. G., CONACYT grant U47366-F to E. V.-S., and UNAM-PAPIIT grant 110606 to J. B.-P. The research of M. S. was funded under the Programme for Research in Third Level Institutions (PRTL) administered by the Irish Higher Education Authority under the National Development Plan and with partial support from the European Regional Development Fund.

REFERENCES

- Alves, J., Lada, C., & Lada, E. 2001, *Nature*, 409, 159
- Ballesteros-Paredes, J., & Hartmann, L. 2007, *Rev. Mex. AA*, 43, 123
- Ballesteros-Paredes, J., Hartmann, L., & Vázquez-Semadeni, E. 1999a, *ApJ*, 527, 285
- Ballesteros-Paredes, J., Klessen, R. S., & Vázquez-Semadeni, E. 2003, *ApJ*, 592, 188
- Ballesteros-Paredes, J., Vázquez-Semadeni, E., & Scalo, J. 1999b, *ApJ*, 515, 286
- Bonnor, W. B. 1956, *MNRAS*, 116, 351
- Briceño, C., et al. 2001, *Science*, 291, 93
- Caselli, P., Benson, P. J., Myers, P. C., & Tafalla, M. 2002, *ApJ*, 572, 238
- Chandrasekhar, S. 1981, *Hydrodynamic and Hydromagnetic Stability* (New York: Dover)
- di Francesco, J., Evans, N. J., II, Caselli, P., Myers, P. C., Shirley, Y., Aikawa, Y., & Tafalla, M. 2007, in *Protostars and Planets V*, ed. B. Reipurth, D. Jewitt, & K. Keil (Tucson: Univ. Arizona Press), 17
- Ebert, R. 1955, *Z. Astrophys.*, 36, 222
- Elmegreen, B. G. 1991, in *The Physics of Star Formation and Early Stellar Evolution*, ed. C. J. Lada & N. D. Kylafis (Dordrecht: Kluwer), 35
- . 1993, *ApJ*, 419, L29
- . 2000, *ApJ*, 530, 277
- Folini, D., & Walder, R. 2006, *A&A*, 459, 1
- Foster, P. N., & Chevalier, R. A. 1993, *ApJ*, 416, 303
- Galván-Madrid, R., Vázquez-Semadeni, E., Kim, J., & Ballesteros-Paredes, J. 2007, *ApJ*, in press (arXiv:0704.3587)
- Goodman, A. A., Barranco, J. A., Wilner, D. J., & Heyer, M. H. 1998, *ApJ*, 504, 223
- Hartmann, L. 2004, in *IAU Symp. 221, Star Formation at High Angular Resolution*, ed. R. Jayawardhana, M. G. Burton, & T. L. Bourke (San Francisco: ASP), 201
- Hartmann, L., Ballesteros-Paredes, J., & Bergin, E. A. 2001, *ApJ*, 562, 852
- Heitsch, F., Mac Low, M.-M., & Klessen, R. F. 2001, *ApJ*, 547, 280
- Hennebelle, P., & Inutsuka, S. 2006, *ApJ*, 647, 404
- Hennebelle, P., & Pérault, M. 1999, *A&A*, 351, 309
- Hennebelle, P., Whitworth, A. P., Gladwin, P. P., & André, P. 2003, *MNRAS*, 340, 870
- Hunter, C. 1977, *ApJ*, 218, 834
- Hunter, J. H., Jr., & Fleck, R. C., Jr. 1982, *ApJ*, 256, 505
- Hunter, J. H., Jr., Sandford, M. T., II, Whitaker, R. W., & Klein, R. I. 1986, *ApJ*, 305, 309
- Kirk, J. M., Ward-Thompson, D., & André, P. 2005, *MNRAS*, 360, 1506
- Klessen, R. S., Ballesteros-Paredes, J., Vázquez-Semadeni, E., & Durán-Rojas, C. 2005, *ApJ*, 620, 786
- Klessen, R. S., Heitsch, F., & Mac Low, M.-M. 2000, *ApJ*, 535, 887
- Lada, C. J., Alves, J. F., & Lombardi, M. 2007, in *Protostars and Planets V*, ed. B. Reipurth, D. Jewitt, & K. Keil (Tucson: Univ. Arizona Press), 3
- Larson, R. B. 1969, *MNRAS*, 145, 271
- Lee, C. W., & Myers, P. C. 1999, *ApJS*, 123, 233
- Lee, C. W., Myers, P. C., & Plume, R. 2004, *ApJS*, 153, 523
- Lee, C. W., Myers, P. C., & Tafalla, M. 1999, *ApJ*, 526, 788
- Lee, S. H., Park, Y.-S., Sohn, J., Lee, C. W., & Lee, H. M. 2007, *ApJ*, 660, 1326
- Li, P. S., Norman, M. L., Mac Low, M.-M., & Heitsch, F. 2004, *ApJ*, 605, 800
- Lou, Y. Q., & Gao, Y. 2006, *MNRAS*, 373, 1610
- Lou, Y. Q., & Wang, W. G. 2006, *MNRAS*, 372, 885
- McKee, C. F., Zweibel, E. G., Goodman, A. A., & Heiles, C. 1993, in *Protostars and Planets III*, ed. E. H. Levy & J. I. Lunine (Tucson: Univ. Arizona Press), 327
- Myers, P. C. 1983, *ApJ*, 270, 105
- Ostriker, E. C., Gammie, C. F., & Stone, J. M. 1999, *ApJ*, 513, 259
- Ostriker, E. C., Stone, J. M., & Gammie, C. F. 2001, *ApJ*, 546, 980
- Penston, M. V. 1969a, *MNRAS*, 144, 425
- . 1969b, *MNRAS*, 145, 457
- Pringle, J. E., Allen, R. J., & Lubow, S. H. 2001, *MNRAS*, 327, 663
- Sasao, T. 1973, *PASJ*, 25, 1
- Schnee, S., Caselli, P., Goodman, A., Arce, H. G., Ballesteros-Paredes, J., & Kuchibhotla, K. 2007, *ApJ*, in press (arXiv:0706.4115)
- Shen, Y., & Lou, Y. Q. 2004, *ApJ*, 611, L117 (SL04)
- Shu, F. 1977, *ApJ*, 214, 488
- Stone, J. M., & Norman, M. L. 1992, *ApJS*, 80, 753
- Tafalla, M., Mardones, D., Myers, P. C., Caselli, P., Bachiller, R., & Benson, P. J. 1998, *ApJ*, 504, 900
- Tafalla, M., Myers, P. C., Caselli, P., & Walmsley, C. M. 2004, *A&A*, 416, 191
- Tafalla, M., Myers, P. C., Caselli, P., Walmsley, C. M., & Comito, C. 2002, *ApJ*, 569, 815
- Tilley, D. A., & Pudritz, R. E. 2004, *MNRAS*, 353, 769
- . 2005, *MNRAS*, submitted (astro-ph/0508562)
- Tohline, J. E., Bodenheimer, P. H., & Christodoulou, D. M. 1987, *ApJ*, 322, 787
- Vázquez-Semadeni, E., Ballesteros-Paredes, J., & Klessen, R. S. 2003, *ApJ*, 585, L131
- Vázquez-Semadeni, E., Gómez, G. C., Jappsen, A. K., Ballesteros-Paredes, J., González, R. F., & Klessen, R. 2007, *ApJ*, 657, 870
- Vázquez-Semadeni, E., Kim, J., Shadmehri, M., & Ballesteros-Paredes, J. 2005, *ApJ*, 618, 344
- Vázquez-Semadeni, E., Passot, T., & Pouquet, A. 1996, *ApJ*, 473, 881
- Vázquez-Semadeni, E., Ryu, D., Passot, T., González, R. F., & Gazol, A. 2006, *ApJ*, 643, 245
- Ward-Thompson, D., André, P., Crutcher, R., Johnstone, D., Onishi, T., & Wilson, C. 2007, in *Protostars and Planets V*, ed. B. Reipurth, D. Jewitt, & K. Keil (Tucson: Univ. Arizona Press), 33
- Whitworth, A., Bate, M. R., Nordlund, Å., Reipurth, B., & Zinnecker, H. 2007, in *Protostars and Planets V*, ed. B. Reipurth, D. Jewitt, & K. Keil (Tucson: Univ. Arizona Press), 459
- Williams, J. P., Myers, P. C., Wilner, D. J., & di Francesco, J. 1999, *ApJ*, 513, L61
- Zuckerman, B., & Palmer, P. 1974, *ARA&A*, 12, 279